



---

International Specialty Conference on Cold-Formed Steel Structures

(1994) - 12th International Specialty Conference on Cold-Formed Steel Structures

---

Oct 18th, 12:00 AM

## The Compressional Behaviour of Perforated Elements

J. Rhodes

Falk D. Schneider

Follow this and additional works at: <https://scholarsmine.mst.edu/isccss>



Part of the [Structural Engineering Commons](#)

---

### Recommended Citation

Rhodes, J. and Schneider, Falk D., "The Compressional Behaviour of Perforated Elements" (1994). *International Specialty Conference on Cold-Formed Steel Structures*. 6. <https://scholarsmine.mst.edu/isccss/12iccfss/12iccfss-session1/6>

This Article - Conference proceedings is brought to you for free and open access by Scholars' Mine. It has been accepted for inclusion in International Specialty Conference on Cold-Formed Steel Structures by an authorized administrator of Scholars' Mine. This work is protected by U. S. Copyright Law. Unauthorized use including reproduction for redistribution requires the permission of the copyright holder. For more information, please contact [scholarsmine@mst.edu](mailto:scholarsmine@mst.edu).

## The Compressional Behaviour of Perforated Elements

Jim Rhodes<sup>1</sup> and Falk D Schneider<sup>2</sup>

### Summary

The behaviour of stub columns with a series of different perforation patterns is examined on the basis of tests. The tests concentrate on plain channel cross sections with perforation layouts systematically varied to examine the effects of perforation position, dimensions and number on the section performance. The application of existing cold formed steel design codes to perforated members is examined on the basis of comparison with the tests, and various modifications to the design codes are considered to take perforations into account. These are described and the comparison with test results is illustrated.

### Introduction

Cold formed steel design codes are in the main not applicable to perforated members, as the background theory and validating experimentation has generally been confined to non-perforated cross sections. In the field of storage racking, however, which accounts for a sizeable proportion of cold formed construction, the uprights are generally perforated, often to a substantial degree. The strut capacity of such members is generally assessed on the basis of tests.

While there has been a substantial number of research projects carried out into the examination of the effects of holes on plate or thin-walled member behaviour, for example (1), (2), (3), these have in the main concentrated on members containing a single hole. Members used in storage racking generally have many perforations. It would be useful, particularly for example in assessing new designs, if analysis methods were available for the evaluation of capacity of multiply perforated members. To this end the investigation described here was initiated.

Although it is not a typical storage racking upright component, the plain channel cross section was selected as the most suitable for an initial investigation such as this because it is easy to manufacture and is composed of stiffened and unstiffened elements which can both be examined for perforation behaviour. The perforations considered were round holes, which could be produced easily, and the variations in perforation geometry were produced by varying hole diameter and hole positions.

### Test Programme

The test programme covered a total of 48 plain channel section stub column specimens, all of 180mm length, and involving three different material thicknesses. The nominal dimensions of the channels were 60mm web, 30mm flanges and material thicknesses of 0.75mm, 1.19mm and 1.6mm.

---

1. Professor, Department of Mechanical Engineering, University of Strathclyde, Glasgow, Scotland.

2. Mechanical Engineering Student, University of Strathclyde and Universitaet Stuttgart, Germany.

For each material thickness all specimens were cut from the same flat sheet of steel to deliver constant material properties. After drilling of the perforations, the specimens were bent on a mechanically operated bending machine and full measurements of the final dimensions were taken.

All specimens were manufactured from plates cut to constant dimensions of 180x120mm. Due to the different thickness and strength of the materials the bending process produced different overall dimensions for the test samples as the sheets were affected by the cold bending to different degrees. In view of this, all calculations and analysis were based on the actual average dimensions obtained from measuring the manufactured specimen.

The relative positions of the perforations were also varied to some degree due to cold bending. In calculations which required knowledge of the perforation locations the actual measured positions were used.

The measured average dimensions of the plain channel section specimens are shown on the next page together with material yield stresses.

For each of the three different material thicknesses the following three series of tests were made:

**Series up.** Two unperforated samples (up) were tested to obtain a basis of reference for the perforated specimens to assist in the investigation of the effects of the perforations, and to evaluate the basic accuracy of the design codes used for analysis by comparing the experimentally obtained results with the theoretically calculated failure loads.

**Series p2.** To investigate the effects of the position of the perforations a series of five different layouts of perforations was tested. Each specimen was perforated at constant intervals with three rows of 2 holes (hence the series name p2) with a diameter of 8mm. Thus the gross cross-sectional area  $A$  was reduced to a net cross-sectional area,  $A_n$ , of 87% of the initial area. The perforations were positioned symmetrically to the central axis of the web (axis of symmetry of the plain channel section). The five layouts of this perforation series and their corresponding labelling are characterized as follows:

- p2-wncl** perforated on the web near the centre line at 2/5 and 3/5 of the width of the web
- p2-wnf** perforated on the web near the flanges at 1/4 and 3/4 of the width of the web
- p2-edg** perforated in the longitudinal edges.
- p2-fnw** perforated on the flanges near the web at 1/3 of the width of the flanges
- p2-fnoe** perforated on the flanges near the outer edges at 2/3 of the width of the flanges

In this series the positions of the perforations were moved in five sequential stages from close to the centre of the web to close to the outside of the flanges. For each layout two identical specimens were manufactured and tested. Thus the total amount of tests within series p2 was ten for each material thickness.

Where the test results of two identical specimens showed large differences or when the test result seemed to deviate substantially from the expected value the test was repeated, i.e. another test sample of identical layout was manufactured and tested. All the test results were treated equally and used to form the arithmetical mean for the overall test result.

**Series p4.** To investigate the effects of the diameter of the holes, i.e. to examine the effects of the reduction of the net cross-sectional area, a series of four different layouts of perforations was carried out. Each test sample was perforated at constant intervals with three rows of 4 holes (hence p4) at identical characteristic positions relative to the centre lines of the elements, ie at the 1/4 and 3/4 positions across the width of the web and at midway across the width of the flanges. The four layouts are as follows:

- p4-4**            perforated with 4 holes of 4mm diameter, net cross-sectional area  $A_n = 87\%$  of A
- p4-8**            perforated with 4 holes of 8mm diameter, net cross-sectional area  $A_n = 74\%$  of A
- p4-12**           perforated with 4 holes of 12mm diameter, net cross-sectional area  $A_n = 61\%$  of A
- p4-16**           perforated with 4 holes of 16mm diameter, net cross-sectional area  $A_n = 48\%$  of A

As mentioned above, the gross cross-sectional area was reduced to net values of 87%, 74%, 61% and 48% of the original values by the incorporation of 4, 8, 12 and 16mm diameter holes respectively. Within series p4 one specimen of each layout was tested, so this series consisted of four tests for each material thickness.

The details of the perforation geometries are shown in Table 1.

Figure 1 shows a set of specimens for series p2 next to an unperforated specimen, and figure 2 shows a set of specimens for series p4.

## Material Properties

The yield stress of the three different materials was experimentally determined using tensile tests according to British Standard BS 18. The tensile specimens were manufactured from the same sheets of material as the plain channel section specimens. For each material thickness three tensile tests were carried out, and the yield strength evaluated as the average of the three test results.

The yield strengths determined in this way are given below, together with the measured average values for the middle surface dimensions  $b_1$  (web width) and  $b_2$  (flange width):-

0.75mm thick material	$Y_s = 184 \text{ N/mm}^2$	$b_1 = 61.15\text{mm}$	$b_2 = 30.82\text{mm}$
1.19mm thick material	$Y_s = 190 \text{ N/mm}^2$	$b_1 = 62.00\text{mm}$	$b_2 = 30.71\text{mm}$
1.60mm thick material	$Y_s = 289 \text{ N/mm}^2$	$b_1 = 61.50\text{mm}$	$b_2 = 30.90\text{mm}$

## The Tests

The specimens were tested on a servo-hydraulic testing machine made by Avery-Denison Limited, Leeds, England (model 7152). This is a combined tension and compression machine with a maximum load capacity of 600kN.

All tests were carried out at a constant end displacement rate of 2.5mm/minute.

The specimens were subjected to uniform axial compression between two plain steel plattens. To align the specimens exactly vertically between the two cross heads of the machine, and to ensure uniformity of the compression, the bottom platten was fitted with a spherical bearing allowing adjustments in all directions. The bearing then was fixed in the position providing the exact vertical alignment by using four adjustable bolts distributed round the bearing. Figure 3 shows a test in progress.

Each test was continued well beyond the ultimate load capacity and concluded only when plastic mechanisms had become well developed. Generally this corresponded to an end displacement of about 3 to 5mm over the total length of the specimens of 180mm.

Typical failure modes of series p2 specimens are illustrated in Figure 4, and Figure 5 shows failed specimens from series p4.

## Test Results and Analysis

The failure loads for the channels tested are summarized in Tables 2 and 3. Where more than one sample of identical layout was tested, the arithmetical mean of the test results has been specified in these tables.

In Tables 2 and 3 theoretical predictions of failure loads based on three different modifications to BS 5950:Part 5 (4) and the European Recommendations (5) are also given. These predictions are obtained by firstly determining the squash load of a non-perforated member according to the design code and then modifying the squash load so evaluated in the light of the perforations. The details of the modifications carried out are as follows:-

To cope with the reduction of the maximum load-bearing capacity due to the perforations the reduction of the load-bearing net cross-sectional area is taken into account. The parts of the assumed undisturbed stress distribution over perforations are simply 'cut out', i.e. they are disregarded. The reduced load-bearing capacity used to predict the failure load of the perforated members in compression is then determined by summing the stresses distributed over the net cross-sectional area.

The three approaches examined differ in the assumption of the undisturbed stress distribution over the cross-section of the plain channel sections:

### Mod 1:

Mod 1 is characterized by the assumption of a constant stress distribution over the whole cross-section, ie a 'smearing' of the effectiveness of the section if local buckling is present. Perforating is regarded as cutting away uniformly loaded parts as shown in Figure 6. Thus the load-bearing capacity is proportional to the net cross-sectional area, i.e. the load-bearing area in the perforated cross-sections.

### Mod 2:

Mod 2 is characterized by the assumption of a constant stress over the effective parts of the cross-section, according to the effective width concept. For the maximum load-bearing capacity, i.e. for failure, this stress equals the yield stress, and the effective parts are assumed to lie adjacent to the corners as shown in Figure 7. Perforating here is regarded as cutting away effective parts of the cross-section. Perforations lying outside effective sections thus are disregarded completely.

### **Mod 3:**

Mod 3 uses a close approximation to the real stress distributions across the section, described by continuous mathematical functions as shown in Figure 8. Here again the parts over perforations are disregarded to calculate the reduced failure load of perforated sections.

### **Effects of Perforation Location**

Test series p2, and the comparisons with each modification of the British and European design documents are illustrated in Figures 9 to 14. The tests show that in the case of slender cross sections, which are substantially affected by local buckling, the incorporation of perforations in the corners has a greater weakening effect than the same perforations at other locations. Mod 1, which 'smears' the effectiveness, does not take account of the position of the perforations, and is thus not equipped to deal with the problem with complete satisfaction. Mod 2 and Mod 3 both take account of the positions of the perforations, and are superior to Mod 1. The best results are given by Mod 3, but this requires a greater amount of labour than Mod 2, and both methods could be considered satisfactory. In comparison of the design codes, BS 5950:Part 5 and the modifications based on this code would appear to be slightly more accurate than the European Recommendations over the range considered, but at the expense of being less conservative, and in some cases overestimating the capacity.

### **Effects of Perforation Magnitudes**

The results of test series p4, and comparisons with the modified design analysis procedures, are shown in Figures 15 to 17. In Figure 15 the three different modifications of the European Recommendations are shown, together with mod 3 for BS 5950:Part 5. The differences between the results for the different modifications are not substantial, and in Figures 16 and 17 only mod 3 for both codes is shown.

From these figures it is evident that the percentage reduction in capacity of the perforated cross sections is, in general, less than the percentage reduction in nett cross sectional area. For the 0.75mm and 1.19mm thick sections, which suffer substantial local buckling, the percentage reduction in capacity is substantially less than the percentage reduction in nett area. For the 1.6mm thick specimens, which suffer less local buckling, the percentage reduction in capacity is closer to the percentage reduction in nett area.

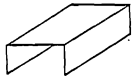
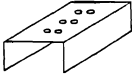
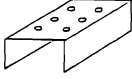

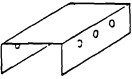
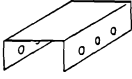
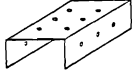
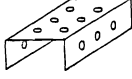
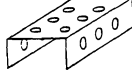
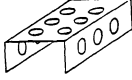
### **Summary**

The test results show clearly that the effects of perforations on member load capacity depend on the location and size of the perforations. It would appear that for members with cross sections which are relatively compact, ie which are not prone to local buckling, that the load capacity can be estimated from the product of the yield stress and the minimum cross sectional area. For members which are subject to local buckling the methods described by mod 2 and mod 3 give conservative estimates of the stub column capacity.

On the basis of the results it can be postulated that safe estimates of stub column load capacity can be obtained for perforated members by initially evaluating the load capacity of a corresponding perforated member and thereafter deducting the loads which would have been carried in the perforated regions.

**References**

1. Yu, W. W. and Davis, C. S. "Buckling behaviour and post-buckling strength of perforated stiffened compression elements", Proc First Specialty Conference on Cold-Formed Steel Structures, 1971
2. Ritchie, D. and Rhodes, J. "Buckling and postbuckling behaviour of plates with holes", Aero. Quarterly, Vol. XXVI, Nov. 1975, pp 281-296.
3. Narayanan, R. and Chow, F. Y. "Ultimate capacity of uniaxially compressed perforated plates", Thin-Walled Structures, Vol 2, No3, 1984, pp 241-264.
4. BS5950:Part 5. "Code of practice for the Design of Cold Formed Sections". British Standards Institution, 1987.
5. "European Recommendations for the Design of Light gauge Steel Members." ECCS, 1986

Label	Sketch	N° of Tests	N° and $\emptyset$ of Holes	Net Cr.-S. Area	Characteristical Position of Perforation
up		2	—	100%	—
p2-wncf		2	2 x 8mm	87%	"web near centre line", at 2/5 and 3/5 the width of the web
p2-wnf		2	2 x 8mm	87%	"web near flanges", at 1/4 and 3/4 the width of the web
p2-edg		2	2 x 8mm	87%	"in the longitudinal edges"
p2-fnw		2	2 x 8mm	87%	"flanges near web", at 1/3 the width of the flanges
p2-fnoe		2	2 x 8mm	87%	"flanges near outer edges", at 2/3 the width of the flanges
p4-4		1	4 x 4mm	87%	at 1/4 and 3/4 the width of the web and at 1/2 the width of the flanges
p4-8		1	4 x 8mm	74%	at 1/4 and 3/4 the width of the web and at 1/2 the width of the flanges
p4-12		1	4 x 12mm	61%	at 1/4 and 3/4 the width of the web and at 1/2 the width of the flanges
p4-16		1	4 x 16mm	48%	at 1/4 and 3/4 the width of the web and at 1/2 the width of the flanges

**TABLE 1. Details of Perforation Geometries for the Sections Tested.**

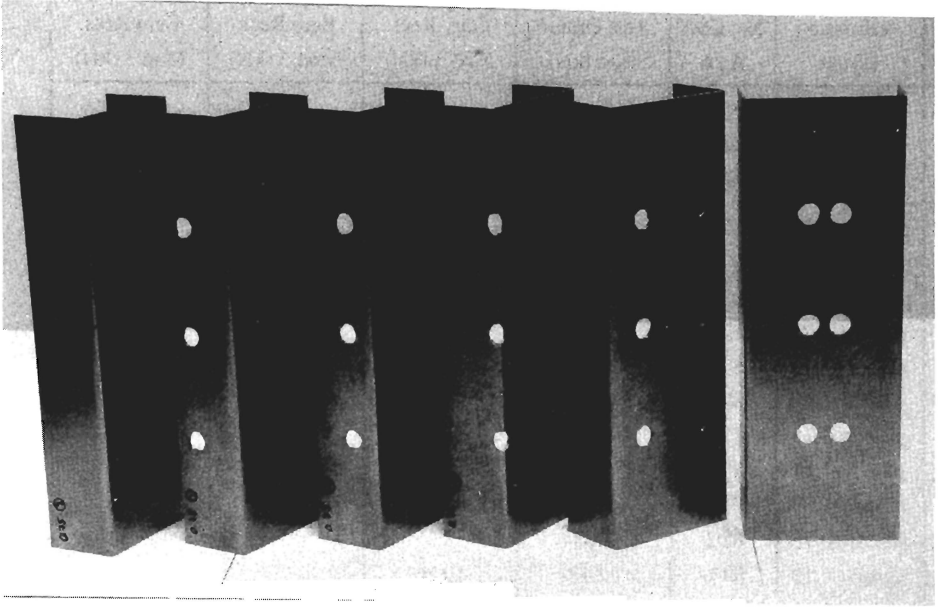


Perforation Layout	Net CSA $A_p/A$	Test Failure load (kN)	BS 5950 Mod 1 (kN)	BS 5950 Mod 2 (kN)	BS 5950 Mod 3 (kN)
up-0.75	100%	9.38	9.88	9.88	9.88
up-1.19	100%	22.90	23.6	23.6	23.6
up-1.60	100%	48.75	50.87	50.87	50.87
p2-wnc1-0.75	87%	9.03	8.60	9.88	9.20
p2-wnc1-1.19	87%	21.90	20.51	20.58	20.64
p2-wnc1-1.60	87%	47.75	44.25	43.47	44.34
p2-wnf-0.75	87%	8.88	8.60	8.19	8.61
p2-wnf-1.19	87%	20.28	20.51	19.96	20.36
p2-wnf-1.60	87%	46.50	44.25	43.47	44.00
p2-edg-0.75	87%	7.85	8.60	7.29	7.33
p2-edg-1.19	87%	19.05	20.51	19.18	19.19
p2-edg-1.60	87%	47.08	44.25	41.95	42.01
p2-fnw-0.75	87%	8.83	8.60	7.67	8.06
p2-fnw-1.19	87%	22.10	20.51	19.96	20.23
p2-fnw-1.60	87%	45.00	44.25	43.47	43.93
p2-fnoe-0.75	87%	9.35	8.60	9.80	9.04
p2-fnoe-1.19	87%	21.55	20.51	20.06	20.96
p2-fnoe-1.60	87%	49.38	44.25	43.47	45.04
p4-4-0.75	87%	9.00	8.60	7.87	8.52
p4-4-1.19	87%	21.40	20.51	19.96	20.44
p4-4-1.60	87%	49.00	44.25	43.45	44.19
p4-8-0.75	74%	8.45	7.31	6.46	7.15
p4-8-1.19	74%	20.00	17.45	16.34	17.33
p4-8-1.60	74%	41.00	37.64	36.05	37.50
p4-12-0.75	61%	7.80	6.03	5.35	5.81
p4-12-1.19	61%	17.30	14.38	12.72	14.24
p4-12-1.60	61%	34.50	31.02	28.65	30.83
p4-16-0.75	48%	6.45	4.74	4.25	4.50
p4-16-1.19	48%	15.40	11.32	9.11	11.17
p4-16-1.60	48%	26.00	24.41	21.25	24.20

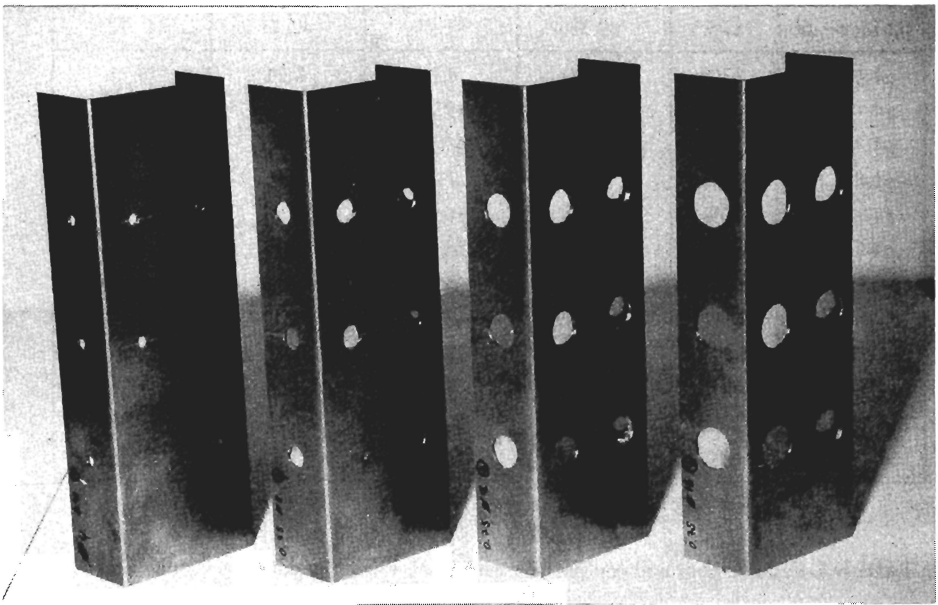
**TABLE 2. Failure loads and comparisons with BS 5950:Part 5 based analysis.**

Perforation layout	Net CSA $A_n/A$	Test Failure load (kN)	Euro. Recs. Mod 1 (kN)	Euro Recs. Mod 2 (kN)	Euro Recs. Mod 3 (kN)
up-0.75	100%	9.38	9.60	9.60	9.60
up-1.19	100%	22.90	22.14	22.14	22.14
up-1.60	100%	48.75	47.94	47.94	47.94
p2-wnc1-0.75	87%	9.03	8.35	9.60	8.76
p2-wnc1-1.19	87%	21.90	19.26	19.17	19.23
p2-wnc1-1.60	87%	47.75	41.71	40.55	41.30
p2-wnf-0.75	87%	8.88	8.35	7.57	8.23
p2-wnf-1.19	87%	20.28	19.26	18.52	18.95
p2-wnf-1.60	87%	46.50	41.71	40.55	40.99
p2-edg-0.75	87%	7.85	8.35	7.00	7.05
p2-edg-1.19	87%	19.05	19.26	17.74	17.88
p2-edg-1.60	87%	47.08	41.71	39.03	39.06
p2-fnw-0.75	87%	8.83	8.35	7.39	7.84
p2-fnw-1.19	87%	22.10	19.26	18.52	18.94
p2-fnw-1.60	87%	45.00	41.71	40.55	41.30
p2-fnoe-0.75	87%	9.35	8.35	9.60	8.98
p2-fnoe-1.19	87%	21.55	19.26	20.02	20.04
p2-fnoe-1.60	87%	49.38	41.71	42.43	43.22
p4-4-0.75	87%	9.00	8.35	8.21	8.25
p4-4-1.19	87%	21.40	19.26	18.52	19.17
p4-4-1.60	87%	49.00	41.71	40.55	41.53
p4-8-0.75	74%	8.45	7.10	6.55	6.90
p4-8-1.19	74%	20.00	16.38	14.90	16.21
p4-8-1.60	74%	41.00	35.47	33.15	35.15
p4-12-0.75	61%	7.80	5.85	5.35	5.59
p4-12-1.19	61%	17.30	13.50	11.43	13.27
p4-12-1.60	61%	34.50	29.94	25.76	28.81
p4-16-0.75	48%	6.45	4.61	4.25	4.31
p4-16-1.19	48%	15.40	10.62	8.72	10.38
p4-16-1.60	48%	26.00	23.01	19.31	22.55

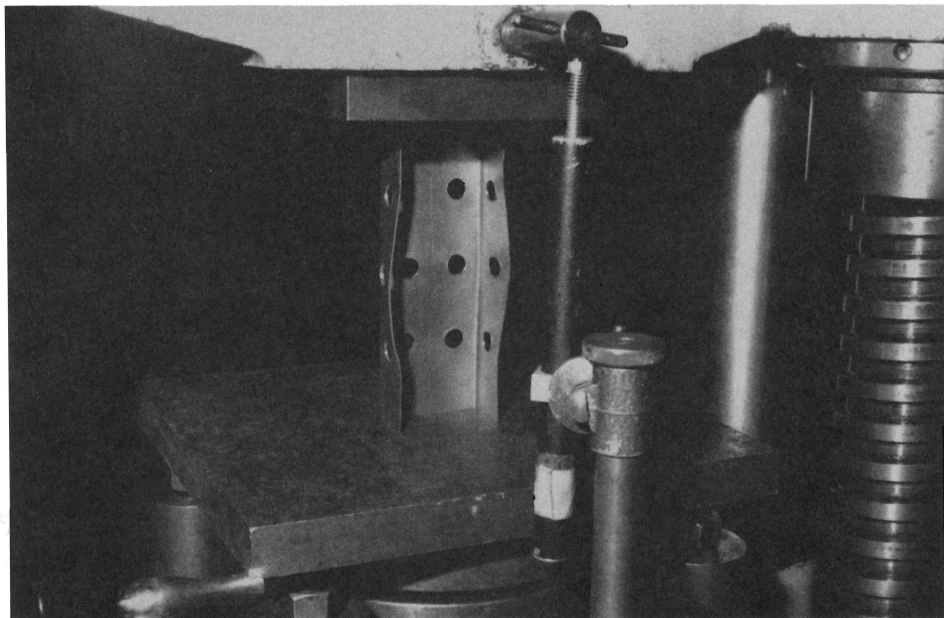
**TABLE 3. Failure loads and comparison with Euro-Recommendations based analysis.**



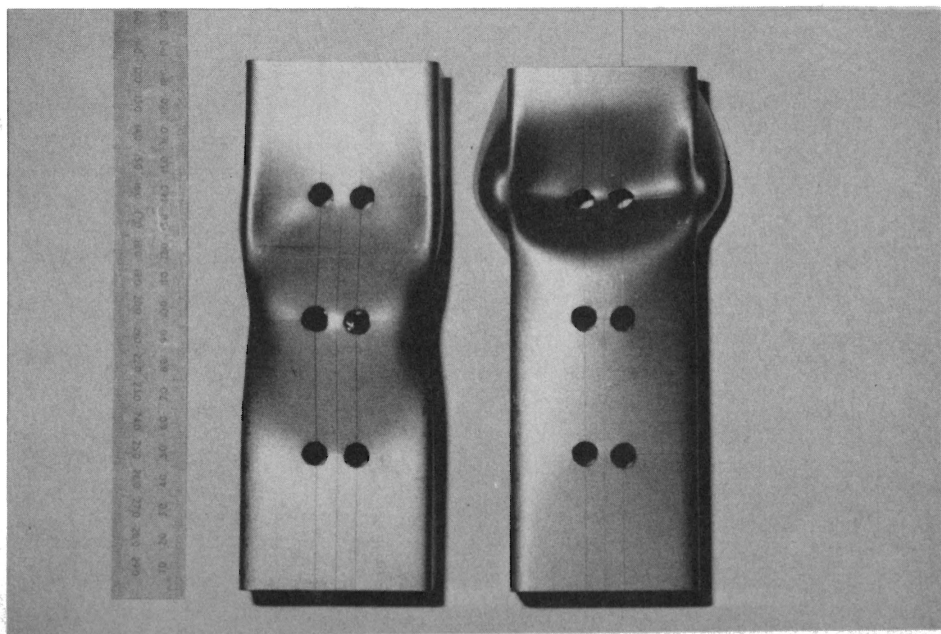
**FIGURE 1. Typical Specimens for Test Series p2.**



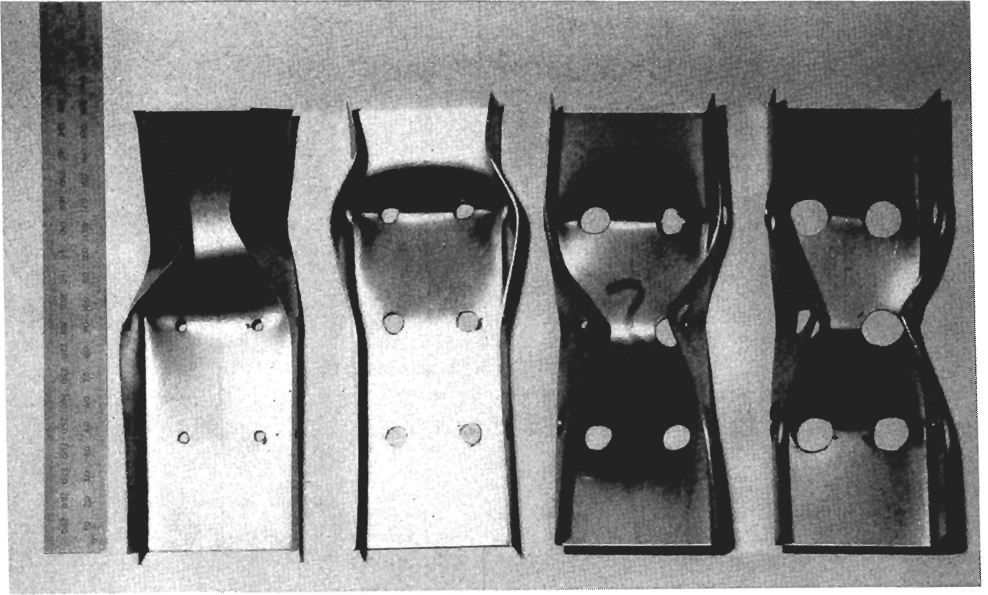
**FIGURE 2. Typical Specimens for Test Series p4.**



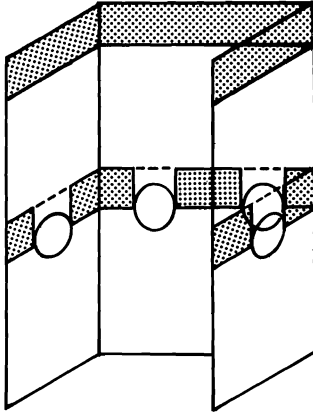
**FIGURE 3. Test in progress.**



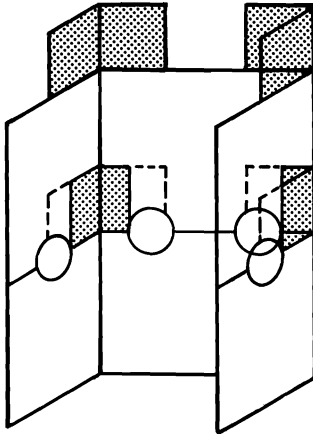
**FIGURE 4. Typical Failed Specimens from Test Series p2.**



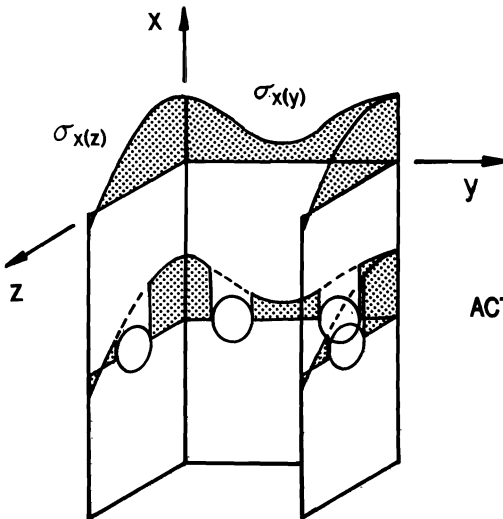
**FIGURE 5. Typical Failed Specimens from Test Series p4.**



**FIGURE 6**  
**MOD 1 - BASED ON**  
**CONSTANT STRESS DISTRIBUTION**



**FIGURE 7**  
**MOD 2 - BASED ON**  
**EFFECTIVE WIDTH CONCEPT**



**FIGURE 8**  
**MOD 3 - BASED ON**  
**ACTUAL STRESS DISTRIBUTION**

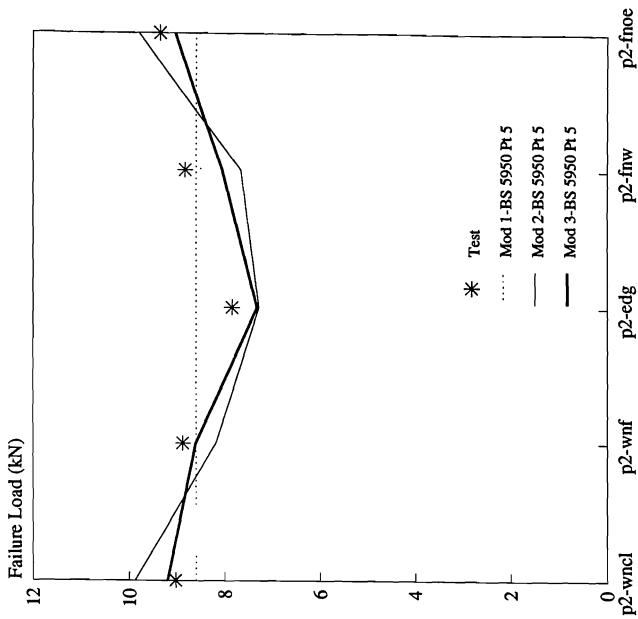


Figure 10. Effects of Perforation Position on Failure Load.  $t=0.75\text{mm}$

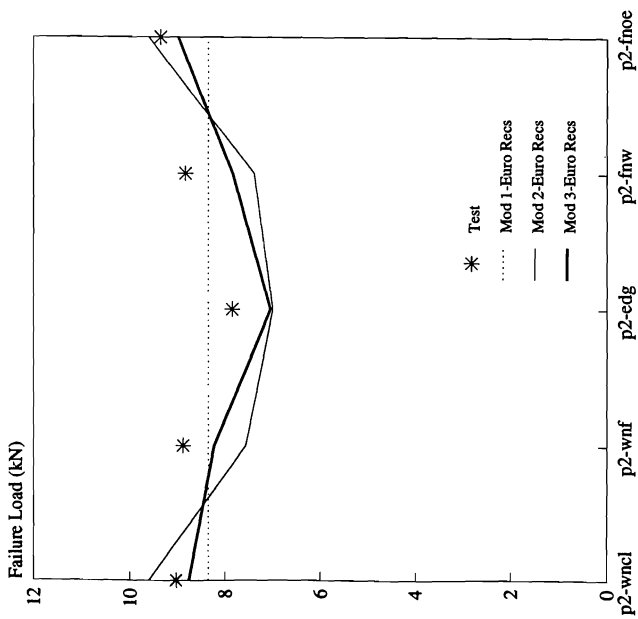


Figure 9. Effects of Perforation Position on Failure Load.  $t=0.75\text{mm}$

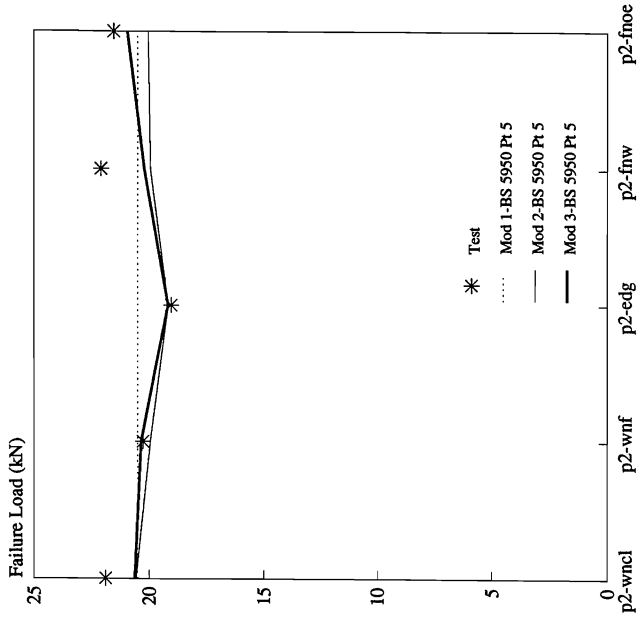


Figure 12. Effects of Perforation Position on Failure Load.  $t=1.19\text{mm}$

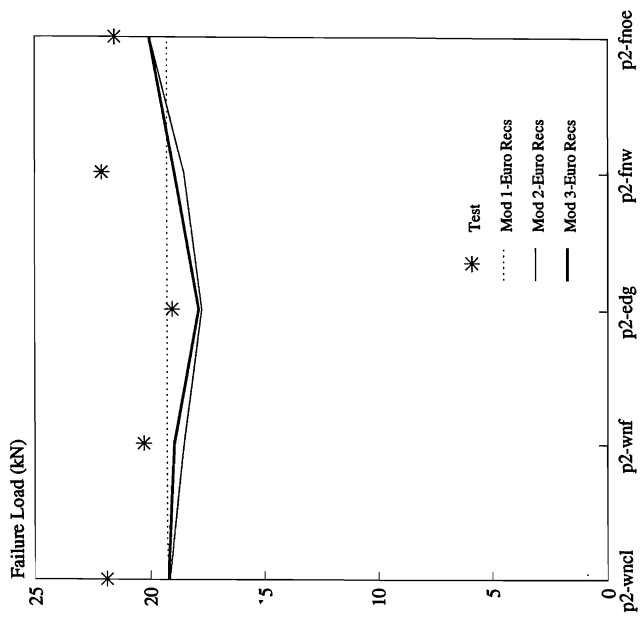


Figure 11. Effects of Perforation Position on Failure Load.  $t=1.19\text{mm}$



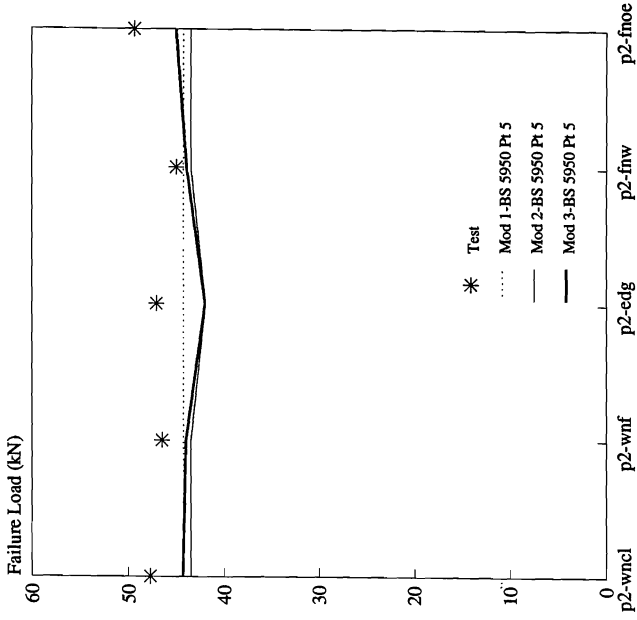


Figure 14. Effects of Perforation Position on Failure Load.  $t=1.60\text{mm}$

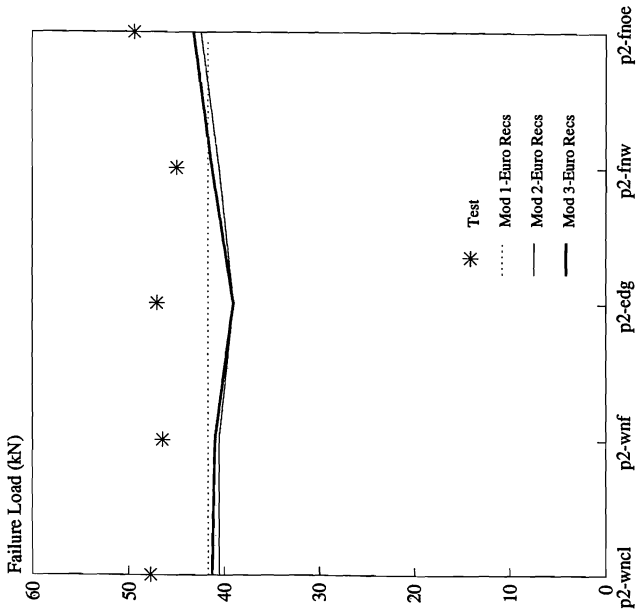


Figure 13. Effects of Perforation Position on Failure Load.  $t=1.60\text{mm}$

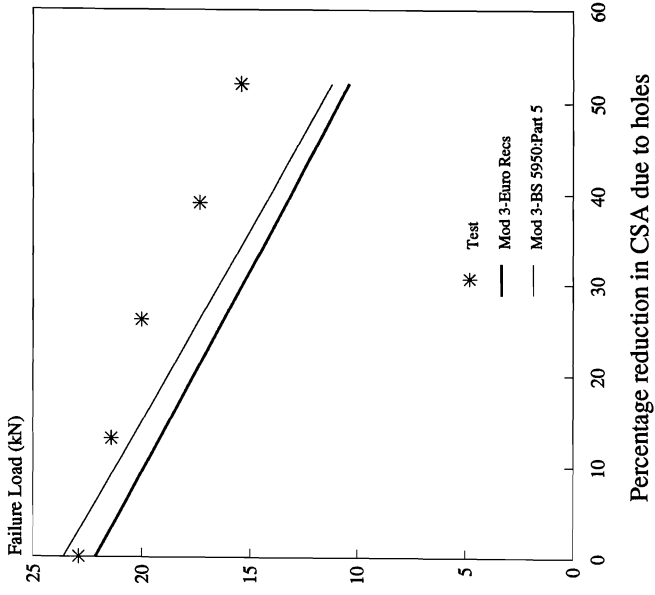


Figure 15. Effects of Perforation Size on Failure Load.  $t=0.75\text{mm}$

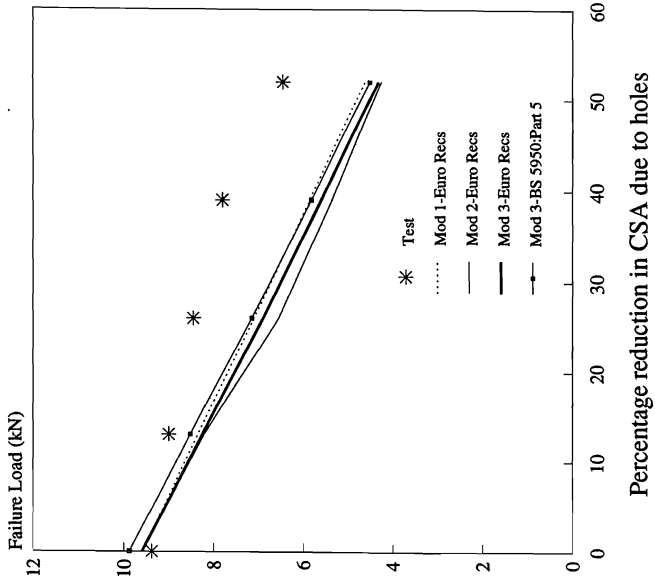


Figure 16. Effects of Perforation Size on Failure Load.  $t=1.19\text{mm}$

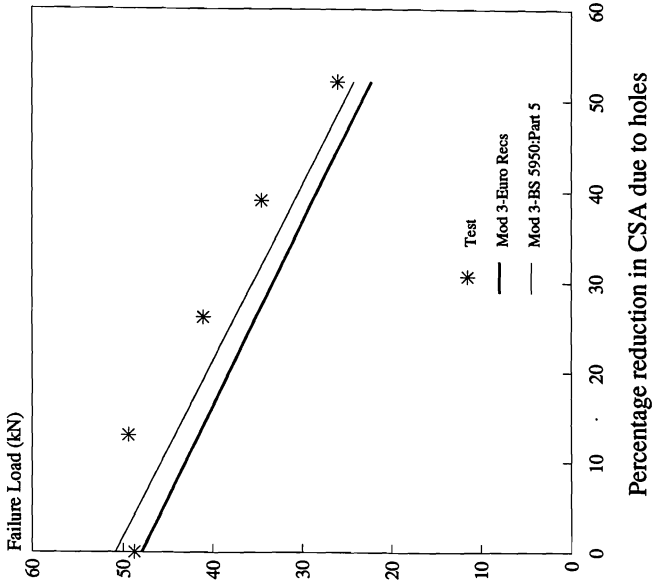


Figure 17. Effects of Perforation Size on Failure Load.  $t=1.6\text{mm}$